

Marshall University

Marshall Digital Scholar

Theses, Dissertations and Capstones

2021

The U-Net-based Active Learning Framework for Enhancing Cancer Immunotherapy

Vishwanshi Joshi
joshi12@marshall.edu

Follow this and additional works at: <https://mds.marshall.edu/etd>



Part of the [Digital Communications and Networking Commons](#), [Diseases Commons](#), [Numerical Analysis and Scientific Computing Commons](#), [Oncology Commons](#), and the [OS and Networks Commons](#)

Recommended Citation

Joshi, Vishwanshi, "The U-Net-based Active Learning Framework for Enhancing Cancer Immunotherapy" (2021). *Theses, Dissertations and Capstones*. 1352.
<https://mds.marshall.edu/etd/1352>

This Thesis is brought to you for free and open access by Marshall Digital Scholar. It has been accepted for inclusion in Theses, Dissertations and Capstones by an authorized administrator of Marshall Digital Scholar. For more information, please contact zhangj@marshall.edu, beachgr@marshall.edu.

**THE U-NET-BASED ACTIVE LEARNING FRAMEWORK FOR ENHANCING
CANCER IMMUNOTHERAPY**

A thesis submitted to
the Graduate College of
Marshall University
In partial fulfillment of
the requirements for the degree of
Master of Science

In
Computer Science
by

Vishwanshi Joshi

Approved by

Dr. Husnu Narman, Committee Chairperson

Dr. Sanghoon Lee

Dr. Haroon Malik

Marshall University

May 2021

APPROVAL OF THESIS

We, the faculty supervising the work of Vishwanshi Joshi, affirm that the thesis, *U-Net based Active Learning Framework for Enhancing Cancer Immunotherapy*, meets the high academic standards for original scholarship and creative work established by the M.S. in Computer Science and the Department of Computer Sciences and Electrical Engineering. This work also conforms to the editorial standards of our discipline and the Graduate College of Marshall University. With our signatures, we approve the manuscript for publication.

Husnu S. Narman

Dr. Husnu Narman, Computer Sciences and Electrical Engineering
Committee Chairperson

Mar. 31, 2021

Date


Dr. Sangoon Lee, Computer Sciences and Electrical Engineering
Committee Member

Mar. 26, 2021

Date


Dr. Haroon Malik, Computer Sciences and Electrical Engineering
Committee Member

Mar. 31, 2021

Date

ACKNOWLEDGMENTS

Throughout the writing of this thesis, I have received a great deal of support and assistance.

I would first like to thank my supervisor and mentor Dr. Sanghoon Lee, whose expert knowledge and familiarity with the subject presented me with a vast pool of resources that I could utilize to the best of my requirements. Furthermore, I would like to express my deepest gratitude for supporting me and guiding me throughout my master's program and my thesis. Not only has he supported me to provide resources for my research, his insight into the writing of this thesis has also allowed me to fine-tune my thinking and has alleviated my work to a higher level. I would not have been able to accomplish this thesis without his ever-present support and guidance.

Secondly, I would like to thank Dr. Malik and Dr. Narman for their sincere remarks. Their insightful feedback and support have enabled me to further refine my thesis so that I may be able to develop it into its current state. Their experience with publications and thesis writing has been a valuable resource for me to further refine my writing skills.

Lastly, I would like to thank the ever-present support of my family and friends. They have fostered the intellectual and critical-thinking skills that were required to write this thesis. They have also supported me in both mind and spirit to encourage me to become a better person. Hence, I would like to name both my parents Dr. Nilkamal Joshi and Varsha Joshi to show my sincerest gratitude and declare that I have achieved new heights due to their love and support. Furthermore, the support I received was further supplemented by the assistance provided by my friends, both old and new.

TABLE OF CONTENTS

List of Tables	vi
List of Figures	vii
Abstract	viii
Chapter 1: Introduction	9
1.1 Background	9
1.2 Motivation	10
1.3 Active Learning for Enhancing Immunotherapy	10
1.4 Contributions	11
1.5 Organization of the Thesis	12
Chapter 2: Literature Review	13
2.1 Semantic Segmentation	13
2.2 Convolutional Neural Network	14
2.3 Deep Convolutional Neural Network	16
2.4 U-Net	17
Chapter 3: Whole Slide Images	18
3.1 Whole Slide Imaging	18
3.2 Whole Slide Image Processing	19
Chapter 4: Active Learning and U-net	21
4.1 Active Learning	21
4.2 U-Net-based Active Learning	22

Chapter 5: Performance Analysis	25
5.1 Dataset.....	25
5.2 Results of Active Learning using U-Net.....	25
5.3 Predicting Cancerous Region on Whole Slide Image	30
5.4 Survival Analysis	32
Chapter 6: Conclusion And Future Work	34
6.1 Conclusion.....	34
6.2 Future Works.....	34
References.....	35
Appendix A: Approval letter	44
Appendix B: Acronyms	45

LIST OF TABLES

Table 1: Modified U-Net model summary.....	26
--	----

LIST OF FIGURES

Figure 1: Labeling a Scene by Human Annotator	14
Figure 2: CNN Based Classification on WSIs	15
Figure 3: Semantic Segmentation Using a Deep Convolutional Neural Network.....	16
Figure 4: U-Net Architecture	17
Figure 5: A WSI Scanner	18
Figure 6: A WSI Virtual Slide Viewer	19
Figure 7: Whole Slide Image Processing.....	20
Figure 8: An Example of an Active Learning Process	21
Figure 9: Active Learning Framework on U-Net.	23
Figure 10: AUC-ROC on Random and Active Learning Prediction.	30
Figure 11: Lymphocyte and Tumor Predictions	31
Figure 12: Kaplan-Meier Overall Survival Analysis Over Time.....	33

ABSTRACT

Breast cancer is the most common cancer in the world. According to the U.S. Breast Cancer Statistics, about 281,000 new cases of invasive breast cancer are expected to be diagnosed in 2021 (Smith et al., 2019). The death rate of breast cancer is higher than any other cancer type. Early detection and treatment of breast cancer have been challenging over the last few decades. Meanwhile, deep learning algorithms using Convolutional Neural Networks to segment images have achieved considerable success in recent years. These algorithms have continued to assist in exploring the quantitative measurement of cancer cells in the tumor microenvironment. However, detecting cancerous regions in whole-slide images has been challenging as it requires substantial annotation and training efforts from clinicians and biologists. In this thesis, a notable instructing process named U-Net-based Active Learning is proposed to improve the annotation and training procedure in a feedback learning process by utilizing a Deep Convolutional Neural Networks model. The proposed approach reduces the amount of time and effort required to analyze the whole slide images. During the Active Learning process, highly uncertain samples are iteratively selected to strategically supply characteristics of the whole slide images to the training process using a low-confidence sample selection algorithm. The performance results of the proposed approach indicated that the U-Net-based Active Learning framework has promising outcomes in the feedback learning process as it reaches 88.71% AUC-ROC when only using 64 image patches, while random lymphocyte prediction reaches 84.12% AUC-ROC at maximum.

Keywords: Active Learning; Deep Learning; Convolutional Neural Network; Image Processing; Whole-Slide Image

CHAPTER 1: INTRODUCTION

1.1 Background

Breast cancer is a rapidly growing tumor characterized by uncontrolled proliferation of the breast and often includes ductal and lobular cells of the breast (Joseph et al., 2019). Among all breast cancer types, invasive ductal carcinoma is the most common cancer comprising 50% to 75% of all breast cancer treatments (Khan et al., 2019). This is followed by the prevalence of invasive lobular carcinoma which accounts for 5% to 15% of all diagnoses, and the rarest type of breast cancers are either mixed ductal or lobular carcinoma, or other rare histologies (Luveta et al., 2020).

With the advances in medical devices such as whole slide scanners, cancer diagnosis and treatment have successfully simplified pathology workflow. Whole slide scanners can digitize a glass slide so that doctors can investigate the digitized slides using a computer machine conveniently (Senaras et al., 2018). However, the size of the digitized slides often exceeds 1GB and requires doctors to consume many efforts on diagnosing cancer, interfering with efficient patient care (Kumar et al., 2020).

The recent development of machine learning and deep learning to enhance medical diagnostics has received considerable attention due to their improvement of the speed of computational performance (Serag et al., 2019). In particular, computational image analysis helps doctors to diagnose cancer disease at an early stage, thereby improving the survival of patients.

1.2 Motivation

According to the U.S. Breast Cancer statistics, about 281,000 new cases of invasive breast cancer are expected to be diagnosed in 2021 and about 43,000 women are expected to die from breast cancer in the United States (Smith et al., 2019). Currently, breast cancer is the most common cancer in the world (Altoé et al., 2021). The average risk of a woman in the United States developing breast cancer is about 13% and the death rates resulting from breast cancer is about 2.6% (DeSantis et al., 2017). The death rate of breast cancer is higher than any other cancer type, and early detection and treatment of breast cancer has been an absolute necessity and has been a highly important issue over the last few decades (Siegel et al., 2020). Identifying cancerous regions from whole slide images requires considerable effort from clinicians and biologists (Yao et al., 2020). The purpose of this thesis is to make this process fast and efficient in the hopes of automating the diagnosis of cancer. This aims to help the patient receive treatment on time and increase the survival rate.

1.3 Active Learning for Enhancing Immunotherapy

Precise analysis of whole-slide imaging has significantly advanced understanding of the tumor microenvironment by promoting new strategies for cancer detection. Deep learning algorithms using Convolutional Neural Networks to segment images have achieved considerable success in recent years and have continued to explore the quantitative measurement of cancer cells in the tumor microenvironment (Wang et al., 2019). However, detecting cancerous regions in whole-slide images has been challenging as it requires substantial annotation and training efforts from pathologists.

This challenge can be overcome by implementing Active Learning, a notable instruction process that requires students' feedback to effectively partake in the learning cycle (Carse & McKenna, 2019). This thesis adopted the Active Learning concept by utilizing the semantic segmentation deep Convolutional Neural Networks model called U-Net which would be further integrated with Active Learning framework to improve the annotation and training procedure in a feedback learning process. This reduced the amount of time and effort required to analyze the whole slide images. As an Active Learning strategy, a low-confidence sample selection algorithm was used to improve the learning process. This method selected highly uncertain samples iteratively to supply whole slide images to the training process strategically. The performance results of the proposed approach indicated that the U-Net-based Active Learning method has promising outcomes in the feedback learning process. Moreover, the research demonstrated that prognostic values using the proposed framework presented meaningful survival analysis results.

1.4 Contributions

The contributions of this thesis are as mentioned below:

- i. Presenting a new approach that combines an Active Learning strategy with a machine learning model to analyze whole slide images.
- ii. Predicting cancerous regions using the combination of Active Learning and machine learning model.
- iii. Demonstrating the effectiveness of the presented approach.

1.5 Organization of the Thesis

The following chapters starting from Chapter 2 describe the literature review and the research on various components used during the thesis, such as Semantic Segmentation, Convolutional Neural Networks, Deep Convolutional Neural Networks, and U-Net. In the next chapter, Chapter 3, whole slide image, and their processing is described. In Chapter 4, Active Learning and U-Net workings are explained in detail. Chapter 5 includes the performance analysis with the dataset used, how the method predicts cancer from whole slide images, and the results and findings of the system. Lastly, the thesis is concluded in Chapter 6 with the conclusion and future works.

CHAPTER 2: LITERATURE REVIEW

2.1 Semantic Segmentation

Semantic segmentation is an image analysis technique that labels an image region at the pixel level (Garcia-Garcia et al., 2017). Semantic segmentation has been successfully studied in the field of computer vision and machine learning. Assigning a particular or an interest class label corresponding to each pixel of an image is an important step in the understanding context of the image, such as building blocks, animals, landscapes, and human cells (Arnab & Torr, 2017). Thus, developing a methodology of semantic segmentation has been a prevalent issue in artificial intelligence communities.

An example of semantic segmentation performed by Zhang et al. (2018) is shown in Figure 1. The first row and the third row represent the original images and the second and the last row represent segmentation regions by human annotator labeling a scene such as bed, horse, and landscape. Recent semantic segmentation methods have made significant enhancement in identifying objects in an image by using Convolutional Neural Networks because of their advantages that is, scene semantics can be learned by pixel-wise training (Sharma et al., 2018).

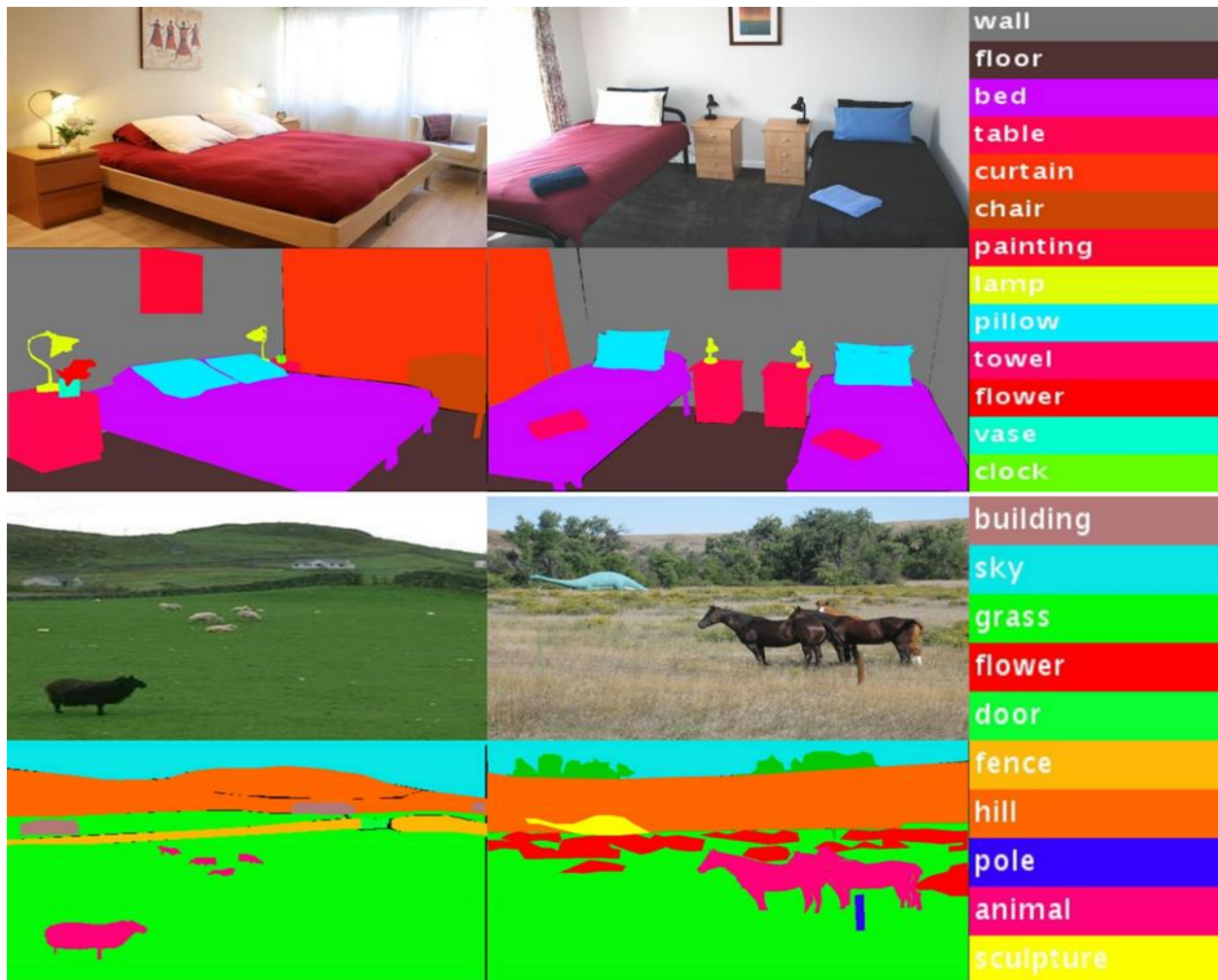


Figure 1: Labeling a Scene by Human Annotator (Zhang et al., 2018).

2.2 Convolutional Neural Network

Convolutional Neural Networks (CNN) to segment images have achieved considerable success in recent years and have helped explore the quantitative measurement of cancer cells in the tumor microenvironment (Tai & Lo, 2018). CNN often uses Deep Neural Networks named after linear mathematical operation between matrices made of complex interconnected layers which help classify the data into various labels (Albawi et al., 2017; LeCun et al., 2004). This method implements convolution procedures on unprocessed data and has had extensive

application utilization in image classification (Guo et al., 2016; Karpathy et al., 2015; Ronao & Cho, 2016). The CNN model consists of a convolutional layer, a pooling layer, and a fully connected layer. These layers are further organized in layers to form a profound structure to facilitate automated pattern or feature derivation in raw data (Ordóñez & Roggen, 2016; Wang et al., 2015). With the aid of various kernel sizes and strides, mapping of features has been done by the convolutional layer and these would then be pooled together to lessen the abundance of links within the convolutional and pooling layers.

CNNs have been widely used with semantic image segmentation, which classifies each pixel into a specific class while separating instances of the same class (Liu et al., 2019). The results of fine-tuned CNNs are transferred to semantic segmentation to get accurate and detailed division (Long et al., 2015). The use of segmentation has been critical in analyzing WSIs and distinguishing different cellular information or diseases (Caicedo et al., 2019). However, the performance of CNN on WSIs poses a drawback due to their size and quantity (Xu et al., 2014). An example of CNN-based tumor classification is shown in Figure 2 which classifies tumors into binary classes such as benign tumors and malignant tumors.

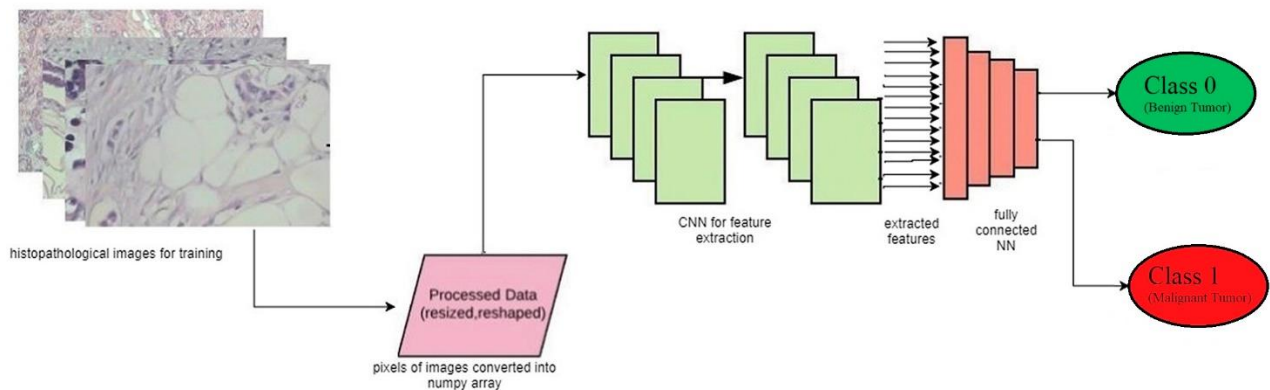


Figure 2: CNN Based Classification on WSIs (Dabeer et al., 2019)

2.3 Deep Convolutional Neural Network

On the other hand, Deep Convolutional Neural Networks (DCNNs) work to improve the performance and computing capabilities of CNNs (Howard, 2013). DCNNs have received much attention in histopathology image analysis (Bejnordi et al., 2016; Yu et al., 2016). Deep-learned features from raw data are now trainable in DCNNs, passing through convolution and pooling layers followed by fully connected layers, and eventually create an optimal model for the histopathological classification task (Hou et al., 2016; Murthy et al., 2017; Sun et al., 2017; Xu et al., 2017). However, DCNNs require a large number of labeled training samples (Ronneberger et al., 2015). Due to the large size of WSIs, labeling becomes a challenging task (Çiçek et al., 2016). Lee et al. (2021) have used DCNNs for processing WSIs, as shown in Figure 3.

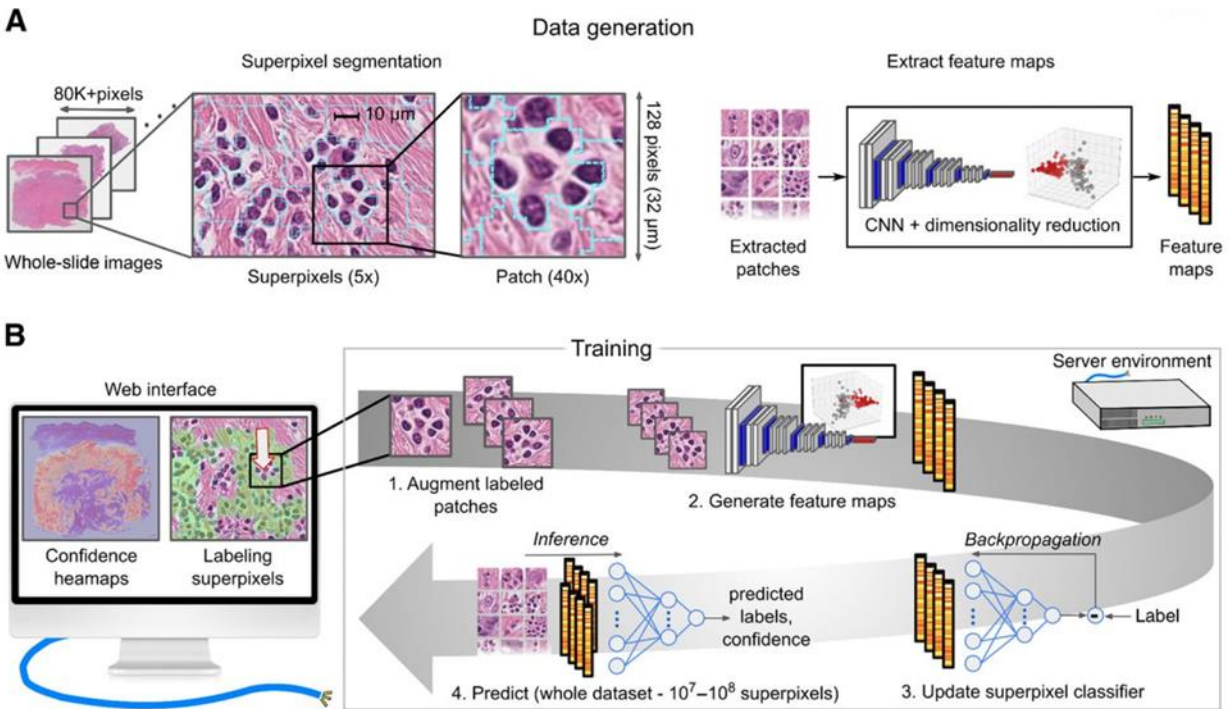


Figure 3: Semantic Segmentation Using a Deep Convolutional Neural Network (Lee et al., 2021)

2.4 U-Net

This is where U-Net, a type of DCNN model specifically developed for biomedical image processing, plays a vital role (Ronneberger et al., 2015). It can not only be fully trained with very few WSIs but can also localize a class label to each pixel (Ronneberger et al., 2015). Some related studies have enabled experts in a collaborating paradigm to provide a feedback learning process (Marée et al., 2016; Xu et al., 2017). However, these studies seem to have overlooked large-scale image analysis. Furthermore, recent studies have predominantly investigated patch-based image analysis rather than pixel-wise image analysis (Amgad et al., 2019; Lee et al., 2019; Lee et al., 2020; Nalisnik et al., 2017). This large-scale image analysis can still require a significant amount of labeling by a pathologist to achieve better results from pixel-wise image analysis. The detailed architecture is shown in Figure 4.

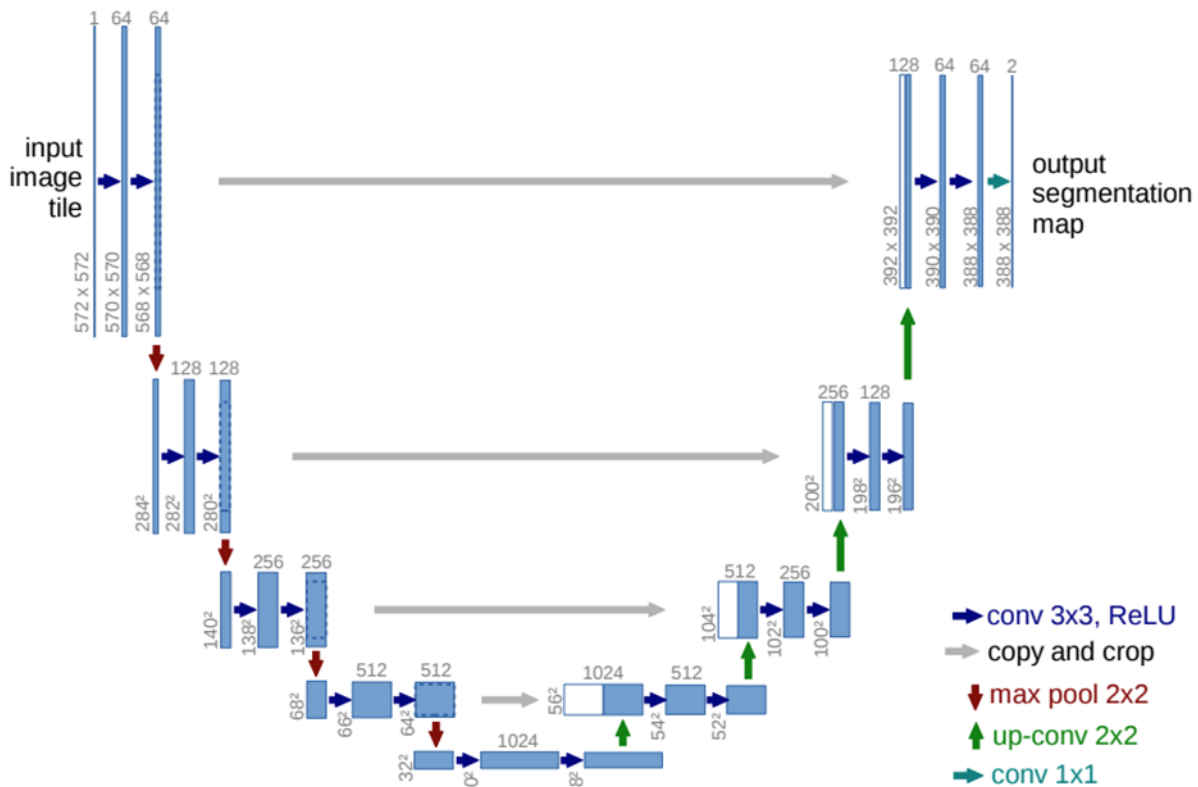


Figure 4: U-Net Architecture (Ronneberger et al., 2015)

CHAPTER 3: WHOLE SLIDE IMAGES

3.1 Whole Slide Imaging

With the help of automated high-resolution whole-slide imaging, analyzing Whole Slide Images (WSIs) has significantly advanced understanding of the tumor microenvironment by promoting new strategies for cancer detection (Hannig et al., 2020). Various types of equipment such as a WSI scanner, WSI viewer, and WSI display have been developed for illuminating precise histopathological image analysis (Dorsa et al., 2020). An example of a WSI scanner is shown in Figure 5 and the pixel-wise slide viewer is shown in Figure 6. Figure 6 represents a slide viewer facilitating pathologist workflow.



Figure 5: A WSI Scanner (Farahani et al., 2015)

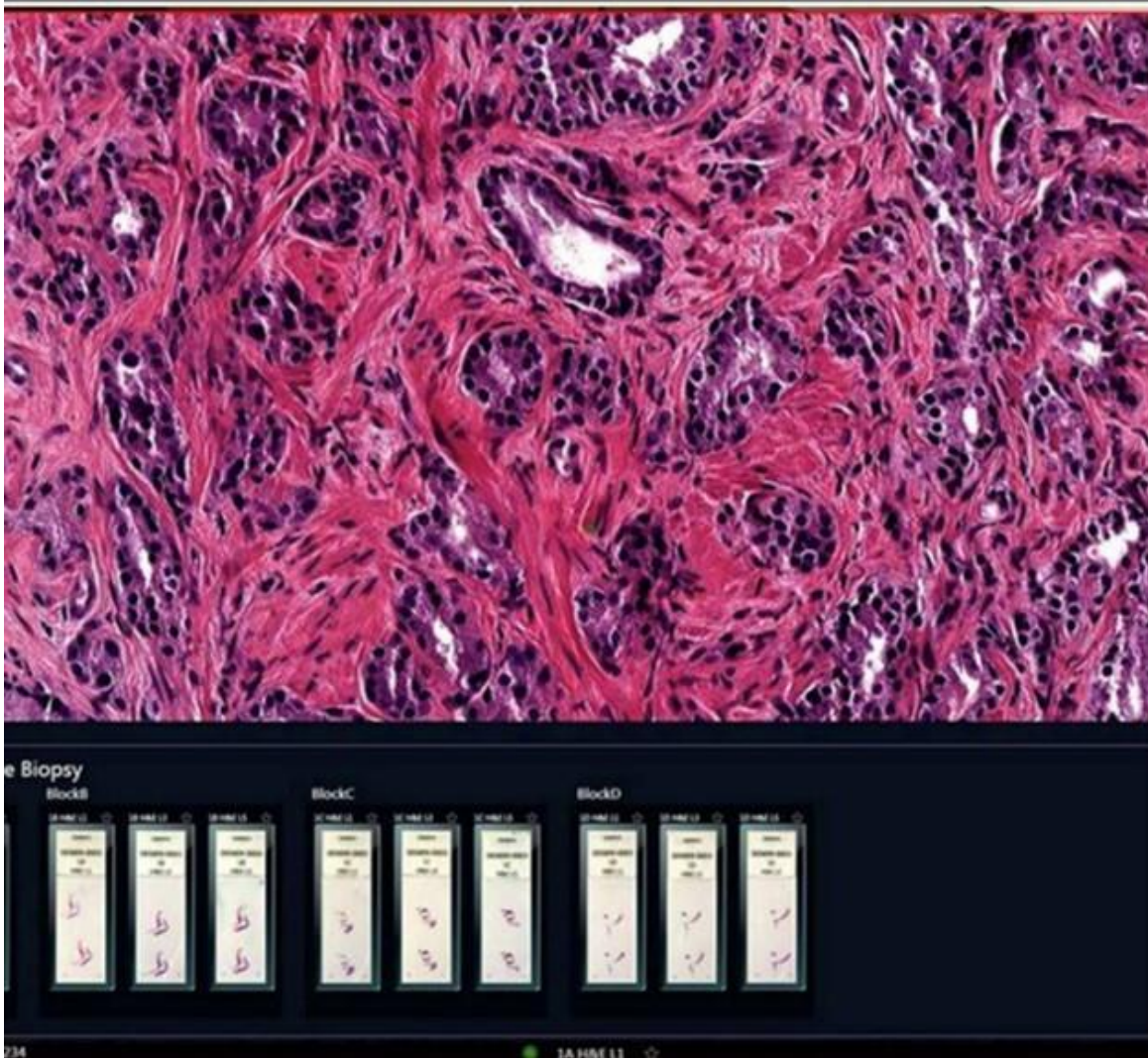


Figure 6: A WSI Virtual Slide Viewer (Farahani et al., 2015)

3.2 Whole Slide Image Processing

A digitized WSI has been widely used for clinical purposes with accurate diagnosis and treatment and is often remotely used for interpreting tissue sections before determining any clinical decision (Coccia, 2020). The tissues on the glass slides to be examined have a short span and could dry out. The glass slides also have to be stored in a secure place where the pathologists can access them efficiently. On the other hand, digitized WSIs can be accessed easily without

any concerns of physical damage (Brust et al., 2018). Although it takes time for a glass slide to be digitized, it is important to be aware of the advantages of digitized slide images.

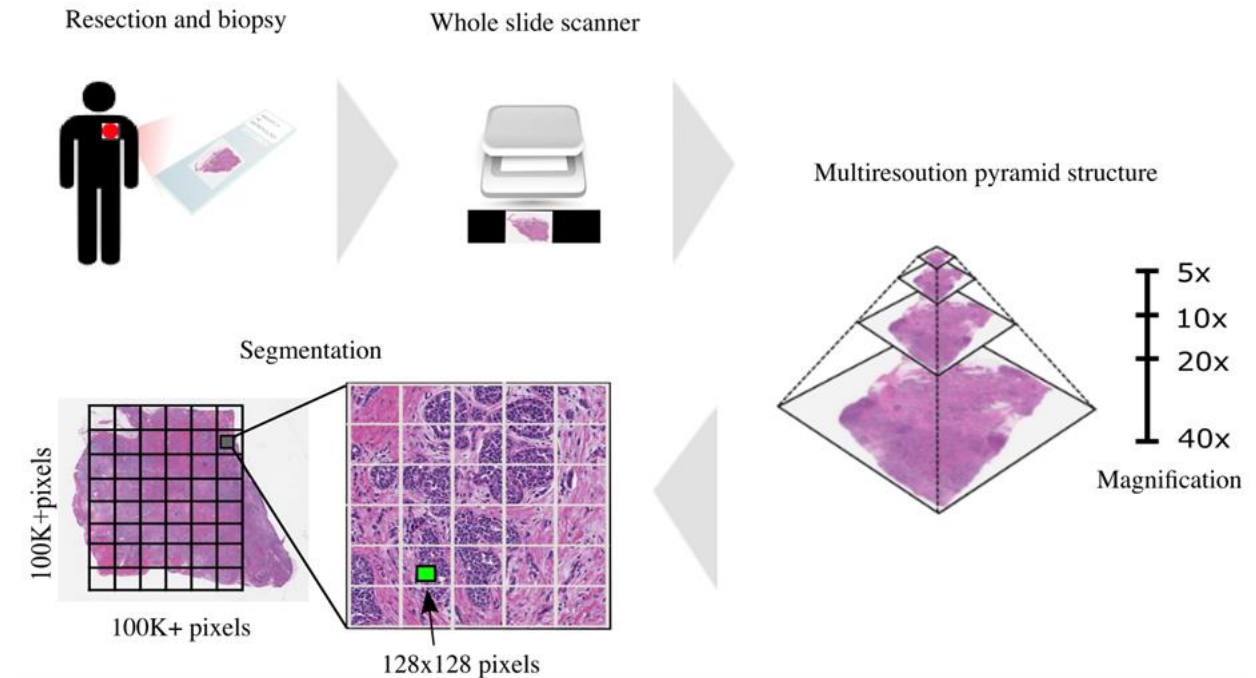


Figure 7: Whole Slide Image Processing

The overall process of the whole slide image processing used in this thesis is shown in Figure 7. A tissue sample of the resection and biopsy obtained from the patient can be stored in a glass slide. By following the formal instructions of the hospital, these glass slides can be scanned by a whole slide scanner generating 5x to 40x magnifications in a large-scale file. In this thesis, we have used these digitized slides to be analyzed in our proposed work. Each whole slide is segmented into several tiles, and the tiles are further segmented into 128x128 sized image patches. We used these image patches for the input of the U-Net model.

CHAPTER 4: ACTIVE LEARNING AND U-NET

4.1 Active Learning

Traditionally, Active Learning has been a well-known teaching method that encourages students to engage in the learning process. In recent years, Active Learning has been a part of machine learning (Wen et al., 2018). The idea of the Active Learning strategy is that an active learner asks a query in the form of unlabeled instances, and then the labeled instances are trained by a machine learning model to generate uncertain instances to be queried by the active learner again (Brust et al., 2018). An example of an Active Learning process is shown in Figure 8.

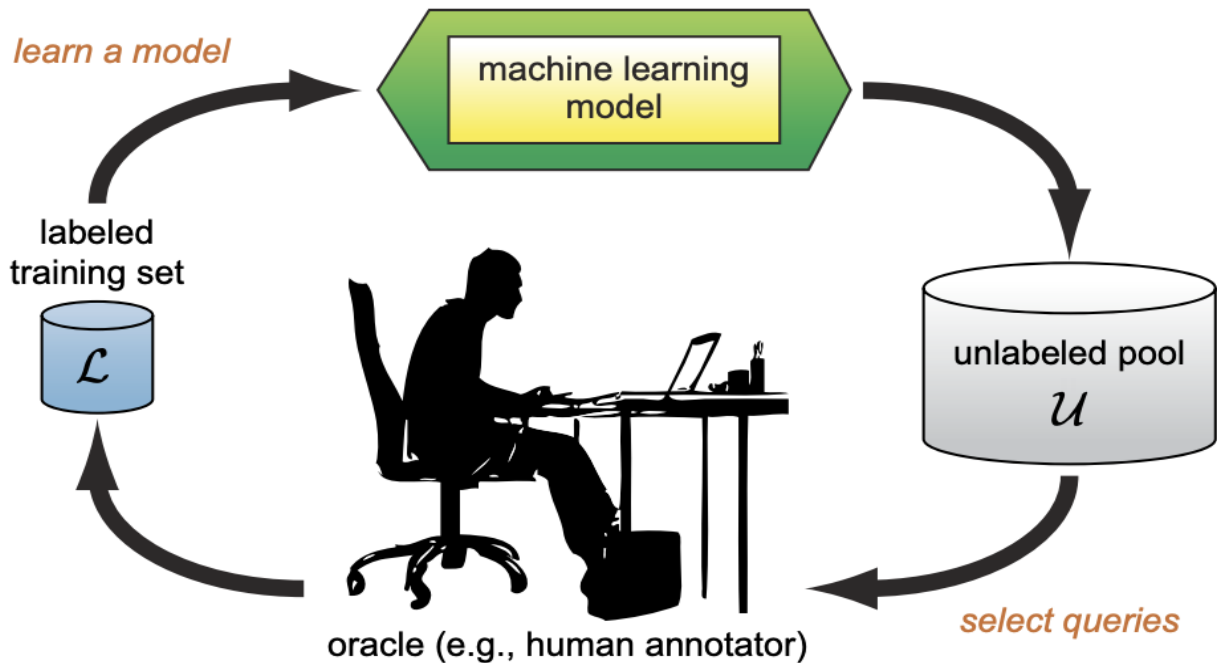


Figure 8: An Example of an Active Learning Process (Settles, 2009)

The number of training samples and manual labeling can be further reduced by applying Active Learning strategies (Settles, 2009). Traditionally, Active Learning is a notable instruction

process that involves students to partake in the learning cycle effectively. Translating the traditional Active Learning strategy to the machine learning concepts would mean actively balancing the training and testing data sets and controlling which set of data would be utilized next for the optimal results (Ertekin et al., 2007; Settles, 2009; Settles, 2011).

4.2 U-Net-based Active Learning

We adopted the fundamental concept of Active Learning in a semantic segmentation deep Convolutional Neural Networks model called U-Net. We propose a U-Net-based Active Learning method for improving the annotating and training procedure in a feedback learning process for reducing the amount of time and effort in the analysis of the whole slide images. We used the square tessellation regions annotated by the expert for training purposes on the U-Net. Prediction probabilities generated by the U-Net model are finally used for the following algorithm 1, low-confidence sample selection. The overall process of the proposed approach is shown in Figure 9.

ALGORITHM 1: Low-confidence Sample Selection

Function selection k , Prob

for all m_{ij} in Prob **do**

 compute $(|2 * \sigma(m_{ij}) - 1|)$;

end

 sort;

 select top k samples;

end

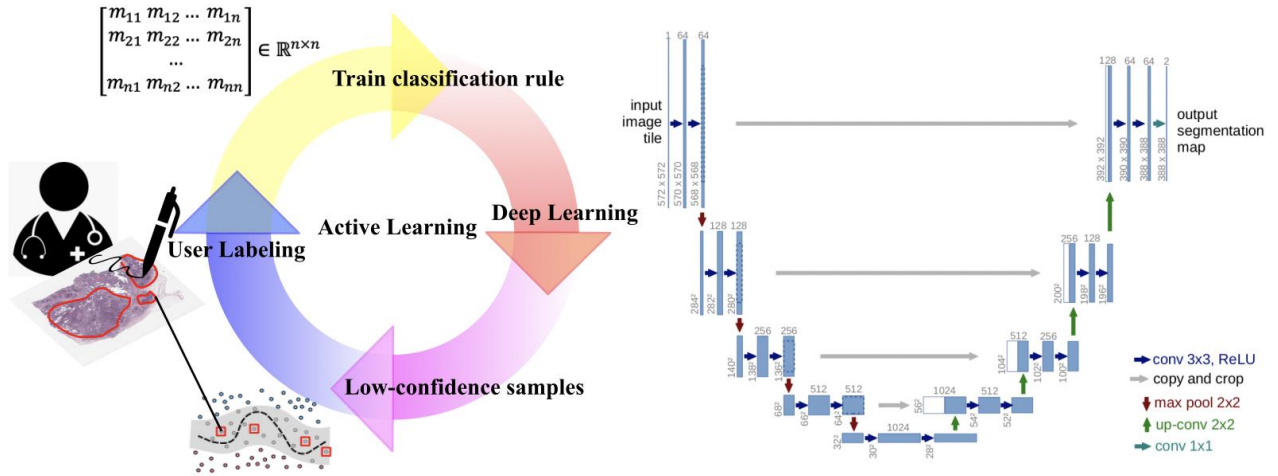


Figure 9: Active Learning Framework on U-Net (Right Image From (Ronneberger et al., 2015)).

In Algorithm 1, Prob represents the prediction probabilities for square tessellation regions generated by U-Net. $m_{ij} \in \mathbb{R}^{n \times n}$ is each prediction probability in the square tessellation region, where i and j are indices for the row and column, and σ is the mean of m_{ij} . Top k samples are selected by sorting the prediction probabilities in ascending order. Algorithm 1 iterates until the prediction meets the user's satisfaction.

Since m_{ij} is a value of probability, the range of this value is between 0 and 1. When it is certain that the WSI contains the cancerous region or the lymphocyte region, the value of $\sigma(m_{ij})$ will be close to 1 as the probability of finding the region will be high. Then the computation result of $|2 * \sigma(m_{ij}) - 1|$ will be $|2*1-1| = 1$. Similarly, when it is certain that the WSI does not contain the cancerous region, the value of $\sigma(m_{ij})$ will be 0 as the probability of not finding the region would be high. The computation result of $|2 * \sigma(m_{ij}) - 1|$ in that case, would be $|2*0-1| = 1$. In both these cases, the value of k is 1, and since they are sorted in ascending order, these types of values will likely be stored at the end.

On the other hand, when it is uncertain that whether the tissue sample has tumor or non-tumor, the value of $\sigma(m_{ij})$ would be close to 0.5. In that case the computation result of $|2 * \sigma(m_{ij}) - 1|$ would be $|2*0.5-1| = 0$. Since the k values are sorted in ascending order, these types of values will be stored towards the top.

The WSIs of the uncertain samples with the k value between 0 to 0.5 are re-evaluated by the clinicians and fed to the system again, making the process quicker.

CHAPTER 5: PERFORMANCE ANALYSIS

5.1 Dataset

In order to measure the performance of the proposed work, we compared the proposed method with the current most used semantic segmentation model, U-Net. In this thesis, the Cancer Genome Atlas Breast Invasive Carcinoma (TCGA-BRCA) dataset (Amgad et al., 2019; Lee et al., 2019; Lee et al., 2020; Nalisnik et al., 2017) was collected for evaluating the proposed method. The dataset was created by using structured crowdsourcing following systematic assignment of tasks with a variety of participants who expertise on breast cancer, and it is freely available. The dataset consists of 151 large regions of interest (ROIs) and a total of 115 TCGA-BRCA images were selected for the validation of the proposed work. The reason why we selected these images is that annotated images have suffered from some problems related to an inter-intra observation problem and these obstacles have made the annotation more difficult. The inter-intra observation problem is a result of conflicting opinions of a label by one or more doctors or pathologists. Inter observation problem would mean two or more individual doctors disagree on the annotated label by another doctor. Intra observation problem would mean an individual doctor disagrees on their annotation later in time. In order to avoid these problems, we have selected these images in which a collaborative annotation was applied on ROIs which would avoid the inter-intra-observation problem.

5.2 Results of Active Learning using U-Net

The performance results on the comparison between the proposed method and the traditional semantic segmentation method: U-Net are described in this section.

We used the annotated TCGA-BRCA images are split into two parts: 73 images for training and 42 images for testing. For each image, 128x128 sized image patches were captured because the input size of the U-Net model is not appropriate for our experiment that detects Tumor-Infiltrating Lymphocytes (TILs) in 40x magnification images. The U-Net model has been initially used on 572x572 sized image patches for the input size, but we modified the input size of the model to 128x128. The modified U-Net summary is shown in Table 1. The first column shows the types of layers used in the U-Net. The second column represents the output shape of the layers. The third column shows the number of parameters and the last column represents the previous layers. The initial input has been 128x128x3 sized such that the height of the image is 128, the width of the image is 128, and the three channels indicate the red, green, and blue color. Our input is (input height) x (input width) x (input channels). When moving from the input convolution layer, the number of images generated by the filters is from 1 to 7 or 8. That is the reason why the U-Net output shape transforms from 128x128x3 to 128x128x16 in Convolutional Layer 1, for example.

Table 1: Modified U-Net Model Summary (Ronneberger et al., 2015)

Layer (type)	Output Shape	Param #	Connected to
input_1 (InputLayer)	[(None, 128, 128, 3)]	0	
lambda (Lambda)	(None, 128, 128, 3)	0	input_1[0][0]
conv2d (Conv2D)	(None, 128, 128, 16)	448	lambda[0][0]
dropout (Dropout)	(None, 128, 128, 16)	0	conv2d[0][0]
conv2d_1 (Conv2D)	(None, 128, 128, 16)	2320	dropout[0][0]
max_pooling2d (MaxPooling2D)	(None, 64, 64, 16)	0	conv2d_1[0][0]
conv2d_2 (Conv2D)	(None, 64, 64, 32)	4640	max_pooling2d[0][0]
dropout_1 (Dropout)	(None, 64, 64, 32)	0	conv2d_2[0][0]

conv2d_3 (Conv2D)	(None, 64, 64, 32)	9248	dropout_1[0][0]
max_pooling2d_1 (MaxPooling2D)	(None, 32, 32, 32)	0	conv2d_3[0][0]
conv2d_4 (Conv2D)	(None, 32, 32, 64)	18496	max_pooling2d_1[0][0]
dropout_2 (Dropout)	(None, 32, 32, 64)	0	conv2d_4[0][0]
conv2d_5 (Conv2D)	(None, 32, 32, 64)	36928	dropout_2[0][0]
max_pooling2d_2 (MaxPooling2D)	(None, 16, 16, 64)	0	conv2d_5[0][0]
conv2d_6 (Conv2D)	(None, 16, 16, 128)	73856	max_pooling2d_2[0][0]
dropout_3 (Dropout)	(None, 16, 16, 128)	0	conv2d_6[0][0]
conv2d_7 (Conv2D)	(None, 16, 16, 128)	147584	dropout_3[0][0]
max_pooling2d_3 (MaxPooling2D)	(None, 8, 8, 128)	0	conv2d_7[0][0]
conv2d_8 (Conv2D)	(None, 8, 8, 256)	295168	max_pooling2d_3[0][0]
dropout_4 (Dropout)	(None, 8, 8, 256)	0	conv2d_8[0][0]
conv2d_9 (Conv2D)	(None, 8, 8, 256)	590080	dropout_4[0][0]
conv2d_transpose (Conv2DTranspo	(None, 16, 16, 128)	131200	conv2d_9[0][0]
concatenate (Concatenate)	(None, 16, 16, 256)	0	conv2d_transpose[0][0] conv2d_7[0][0]
conv2d_10 (Conv2D)	(None, 16, 16, 128)	295040	concatenate[0][0]
dropout_5 (Dropout)	(None, 16, 16, 128)	0	conv2d_10[0][0]
conv2d_11 (Conv2D)	(None, 16, 16, 128)	147584	dropout_5[0][0]
conv2d_transpose_1 (Conv2DTrans	(None, 32, 32, 64)	32832	conv2d_11[0][0]
concatenate_1 (Concatenate)	(None, 32, 32, 128)	0	conv2d_transpose_1[0][0] conv2d_5[0][0]
conv2d_12 (Conv2D)	(None, 32, 32, 64)	73792	concatenate_1[0][0]
dropout_6 (Dropout)	(None, 32, 32, 64)	0	conv2d_12[0][0]
conv2d_13 (Conv2D)	(None, 32, 32, 64)	36928	dropout_6[0][0]

conv2d_transpose_2 (Conv2DTrans	(None, 64, 64, 32)	8224	conv2d_13[0][0]
concatenate_2 (Concatenate)	(None, 64, 64, 64)	0	conv2d_transpose_2[0][0] conv2d_3[0][0]
conv2d_14 (Conv2D)	(None, 64, 64, 32)	18464	concatenate_2[0][0]
dropout_7 (Dropout)	(None, 64, 64, 32)	0	conv2d_14[0][0]
conv2d_15 (Conv2D)	(None, 64, 64, 32)	9248	dropout_7[0][0]
conv2d_transpose_3 (Conv2DTrans	(None, 128, 128, 16)	2064	conv2d_15[0][0]
concatenate_3 (Concatenate)	(None, 128, 128, 32)	0	conv2d_transpose_3[0][0] conv2d_1[0][0]
conv2d_16 (Conv2D)	(None, 128, 128, 16)	4624	concatenate_3[0][0]
dropout_8 (Dropout)	(None, 128, 128, 16)	0	conv2d_16[0][0]
conv2d_17 (Conv2D)	(None, 128, 128, 16)	2320	dropout_8[0][0]
conv2d_18 (Conv2D)	(None, 128, 128, 1)	17	conv2d_17[0][0]
Total params: 1,941,105			
Trainable params: 1,941,105			
Non-trainable params: 0			

Python packages of Tensorflow 1.14 and Keras 1.0 were used for training 73 images and then testing 42 images to determine whether the image patch in each image is Tumor/TILs or not. The performance evaluation results of the proposed Active Learning framework are shown in the following Figure 10. The x-axis represents the number of image patches to be trained in the images and the y-axis represents AUC-ROC curve values. The Receiver Operator Characteristic (ROC) curve is a popular measurement generated by plotting the True Positive Rate (TPR) and the False Positive Rate (FPR). The TPR and the FPR are computed as below:

$$True\ Positive\ Rate = \frac{True\ Positive}{True\ Positive + False\ Negative}$$

$$\text{False Positive Rate} = \frac{\text{False Positive}}{\text{False Positive} + \text{True Negative}}$$

Here, the TPR indicates that the proportion of the image patches with TILs correctly classified, and the FPR indicates that the proportion of the image patches with non-TILs not correctly classified. The area under the curve (AUC) is a well-known metric that shows the rate of correct classification. The AUC is defined as below:

$$AUC = \int_0^1 f(x)dx$$

, where $f(x)$ is the ROC curve above the x-axis. By using the AUC-ROC, we can compare the proposed method with the traditional semantic segmentation method, U-Net.

We performed two experiments for predicting the tumor versus non-tumor and the TILs versus non-TILs, respectively. In order to compare the original U-Net with our approach (U-Net-based Active Learning model), we initially selected 16 random samples from the training dataset consisting of 73 images. Here, the 16 random samples represent the 128x128x3 sized image patches in 73 images. We selected 16 random samples since Active Learning requires a set of initial samples to be selected. Since we are not experts on breast cancer, the initial samples were selected randomly. These samples can be adjusted for further experimentation, but we leave this issue for future research. The number of samples is increased by 16 so a total of 32 samples are used for training. Consequently, by incrementally increasing the sample size, we reached a total of 80 samples to compare the prediction results of the original U-Net model with the prediction results of the U-Net model with Active Learning. This comparison was repeated 10 times and the resultant prediction probabilities of the comparison are shown in Figure 10. The box plot

represents the U-Net random sampling for the tumor in A and lymphocyte in B. The blue line represents U-Net model with Active Learning for the tumor in A and lymphocyte in B.

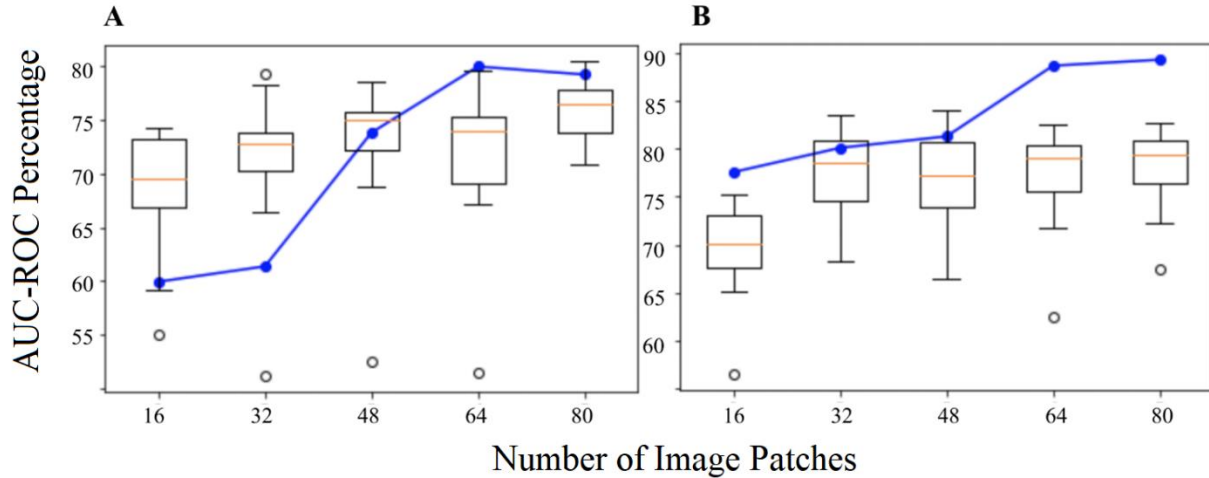


Figure 10: AUC-ROC on Random and Active Learning Prediction.

A. Comparison of Random Tumor Prediction (Boxplot) and Active Learning Tumor Prediction (Blue Line). B. Comparison of Random Lymphocytes Prediction (Boxplot) and Active Learning Lymphocytes Prediction (Blue Line)

As shown in Figure 10, from the two experiments, we found that the proposed Active Learning based on U-Net reaches 88.71% AUC-ROC when only using 64 ROI image patches, while random lymphocyte prediction reaches 84.12% AUC-ROC at maximum. These results show that the proposed method is very effective in predicting tumors and TILs.

5.3 Predicting Cancerous Region on Whole Slide Image

In addition to the performance evaluation, we used the trained model created by the proposed U-Net-based Active Learning for predicting WSIs. The prediction results of the WSIs are shown in Figure 11. A represents the original whole-slide image, and B and C represent the pixel probabilities for lymphocytes and tumors, respectively. D represents a combined B and C

version, where lymphocytes are stained red, and tumors are stained blue. The brighter light in sections B, C, and D, the higher the pixel probabilities are in the images.

Prediction results are shown in Figure 10. A represents the original whole-slide image, and B and C represent the pixel probabilities for lymphocytes and tumors, respectively. The brighter light you see, the higher the pixel probabilities are in the images. D represents a combined B and C version, where lymphocytes are stained red, and tumors are stained blue.

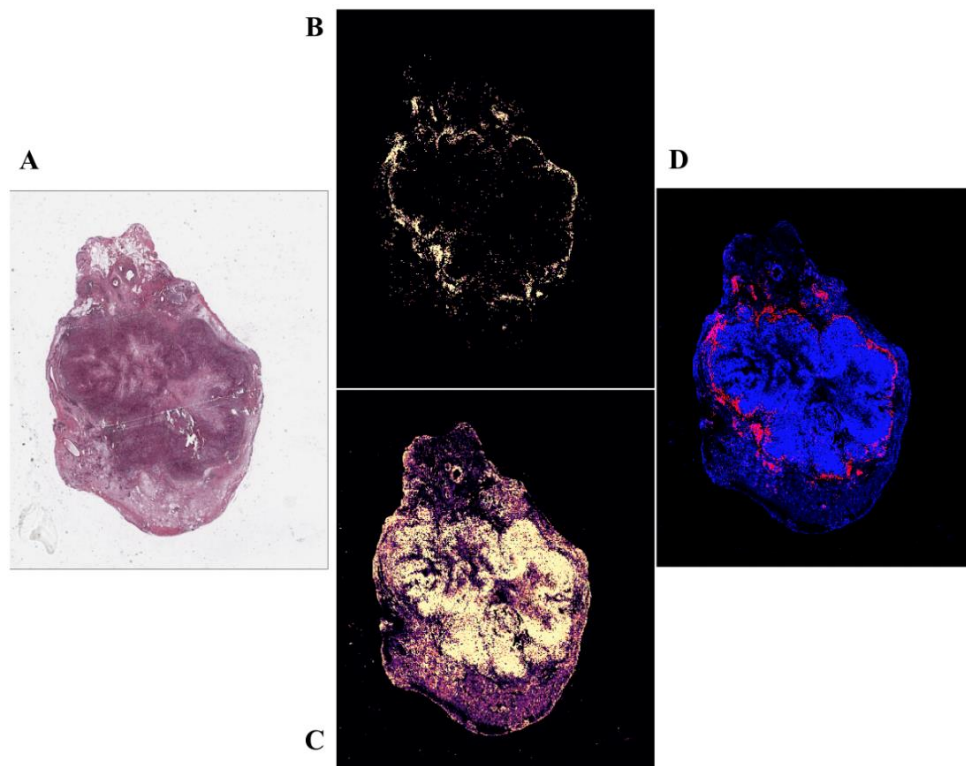


Figure 11: Lymphocyte and Tumor Predictions

Lymphocyte and Tumor Predictions on a Whole Slide Image Using the Proposed Active Learning Framework. A. Original Whole Slide Image. B. Lymphocyte Prediction. C. Tumor Prediction. D. Combined Prediction.

5.4 Survival Analysis

With further development and incorporation of these methods and strategies, significant information can be retrieved such as survival analysis based on WSIs. This is a technique that statistically analyzes the time it takes for an event of interest to occur (Sullivan, 2016; Zhu et al., 2017). This event of interest can be the re-emergence of the disease or death (Sullivan, 2016). Precise Survival Analysis can further advance WSI technologies to enhanced immunotherapy research on cancer with a large amount of medical image data to promote effective therapy for patients with minimum annotating, training data, and computational resources.

The prognostic value of the lymphocyte percentages over the tumor accessed by the proposed Active Learning framework on 100 whole-slide images is presented in Figure 12. We have used the Kaplan-Meier approach for predicting survival probabilities since it avoids change due to the organization of the intervals by re-estimating the survival probability at each instance an event, such as recurrence of the disease or death, is encountered. It is a more accurate measurement of survival probabilities than other methods such as a Life Table approach.

The percentages of the subtypes, lymphocytes-high, and lymphocytes-low were significantly predicted disease progression risk in the cohort (log-rank $p=4.97e-3$). It shows that the survival rate higher where the percentage of lymphocytes is higher, and the survival rate is lower where the percentage of lymphocytes is lower. The log-rank test is used to test the validity of the null hypotheses to compare the frequencies of an event at any point in time among two independent groups using chi-square distribution.

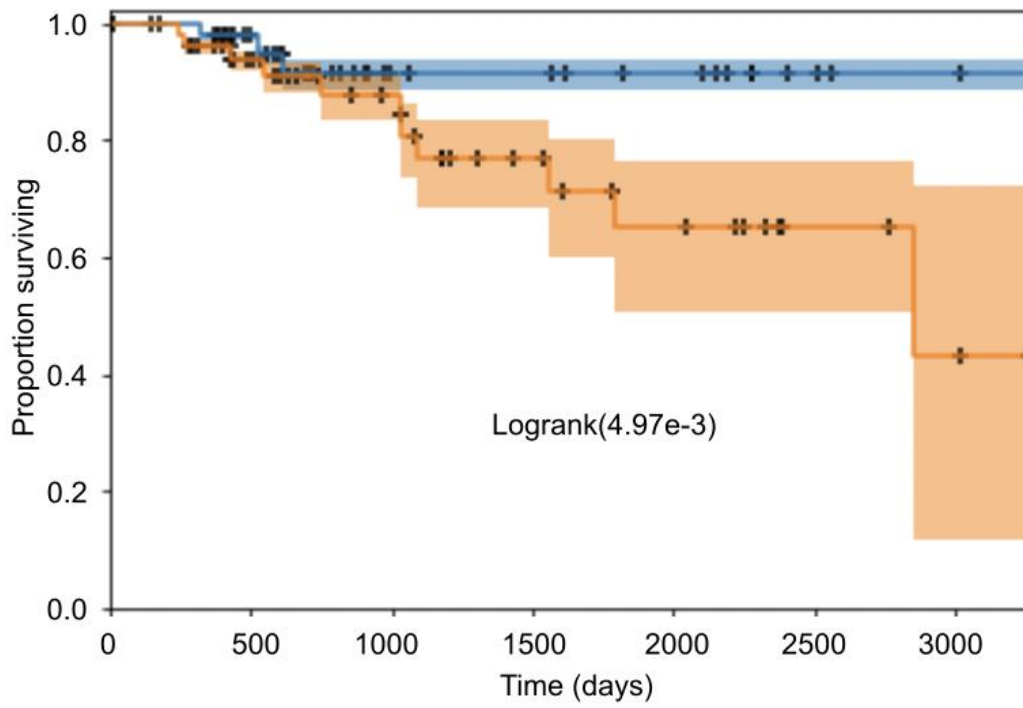


Figure 12: Kaplan-Meier Overall Survival Analysis Over Time (Days).

Stratifications of the Subtypes are Lymphocytes-High (Blue) and Lymphocytes-Low (Orange), Respectively.

CHAPTER 6: CONCLUSION AND FUTURE WORK

6.1 Conclusion

In this thesis, we presented a U-Net-based Active Learning method for improving the annotating and training procedure in a feedback learning process, and thereby reducing the amount of time and effort in analyzing the whole slide images. Our experimental results demonstrate that the proposed framework enhances cancerous region detection performance in a limited number of image patches. Moreover, we found that the prognostic value of the cancerous region's percentages derived from the proposed framework provides insights on survival analysis.

6.2 Future Works

Although the proposed method is efficient and effective in predicting cancer regions, the experiments were limited to specific types of cancers. We plan to extend our Active Learning-based method to other types of cancers such as brain tumors, lung cancer, and pancreatic cancer. Furthermore, our methodology can be expanded to unsupervised methods (Kallenberg et al., 2016; Lee, Farley, et al., 2020).

REFERENCES

- Albawi, S., Mohammed, T. A., & Al-Zawi, S. (2017). *Understanding of a Convolutional Neural Network*. International Conference on Engineering and Technology (ICET).
- Altoé, M. L., Marone, A., Kim, H., Guo, H., Hibshoosh, H., Tejada, M., Crew, K., Accordino, M., Trivedi, M., Kalinsky, K., Hershman, D., & Hielscher, A. (2021). *Total Hemoglobin Changes in the Breast Tumors Volume of Patients Undergoing Neoadjuvant Chemotherapy: A Longitudinal Analysis* (Vol. 11639). *SPIE*.
<https://doi.org/10.1117/12.2583101>
- Amgad, M., Elfandy, H., Hussein, H., Atteya, L. A., Elsebaie, M. A., Abo Elnasr, L. S., Sakr, R. A., Salem, H. S., Ismail, A. F., & Saad, A. M. (2019). Structured crowdsourcing enables convolutional segmentation of histology images. *Bioinformatics*, 35(18), 3461-3467.
<https://doi.org/10.1093/bioinformatics/btz083>
- Arnab, A., & Torr, P. H. (2017). *Pixelwise Instance Segmentation with a Dynamically Instantiated Network*. Proceedings of the IEEE Conference on Computer Vision and Pattern Recognition.
- Bejnordi, B. E., Balkenhol, M., Litjens, G., Holland, R., Bult, P., Karssemeijer, N., & Van Der Laak, J. A. (2016). Automated detection of DCIS in whole-slide H&E stained breast histopathology images. *IEEE Transactions on Medical Imaging*, 35(9), 2141-2150.
<https://doi.org/10.1109/TMI.2016.2550620>
- Brust, C.-A., Käding, C., & Denzler, J. (2018). Active Learning for deep object detection. *arXiv preprint arXiv:1809.09875*. <https://doi.org/arXiv:1809.09875v1>
- Caicedo, J. C., Roth, J., Goodman, A., Becker, T., Karhohs, K. W., Broisin, M., Molnar, C., McQuin, C., Singh, S., & Theis, F. J. (2019). Evaluation of deep learning strategies for

- nucleus segmentation in fluorescence images. *Cytometry Part A*, 95(9), 952-965.
<https://doi.org/10.1002/cyto.a.23863>
- Carse, J., & Mckenna, S.. (2019). Active learning for patch-based digital pathology using convolutional neural networks to reduce annotation costs. In *Transactions on Petri Nets and Other Models of Concurrency XV* (pp. 20–27). https://doi.org/10.1007/978-3-030-23937-4_3
- Çiçek, Ö., Abdulkadir, A., Lienkamp, S. S., Brox, T., & Ronneberger, O. (2016, October). 3D U-Net: learning dense volumetric segmentation from sparse annotation. In *International Conference on Medical Image Computing and Computer-Assisted Intervention* (pp. 424-432). Springer, Cham.
- Coccia, M. (2020). Deep learning technology for improving cancer care in society: New directions in cancer imaging driven by artificial intelligence. *Technology in Society*, 60, 101198. <https://doi.org/10.1016/j.techsoc.2019.101198>
- Dabeer, S., Khan, M. M., & Islam, S. (2019). Cancer diagnosis in histopathological image: CNN based approach. *Informatics in Medicine Unlocked*, 16, 100231.
<https://doi.org/10.1016/j.imu.2019.100231>
- DeSantis, C. E., Ma, J., Goding Sauer, A., Newman, L. A., & Jemal, A. (2017). Breast cancer statistics, racial disparity in mortality by state. *CA: A Cancer Journal for Clinicians*, 67(6), 439-448. <https://doi.org/10.3322/caac.21412>
- Dorsa, Z., Weizhe, L., Samuel, L., Wei-Chung, C., & Weijie, C. (2020). Characterization of color normalization methods in digital pathology whole slide images. *Proc.SPIE*,

- Ertekin, S., Huang, J., Bottou, L., & Giles, L. (2007). *Learning on the Border: Active Learning in Imbalanced Data Classification*. Proceedings of the sixteenth ACM conference on Conference on Information and Knowledge Management,
- Farahani, N., Parwani, A. V., & Pantanowitz, L. (2015). Whole slide imaging in pathology: Advantages, limitations, and emerging perspectives. *Pathology and Laboratory Medicine International*, 7, 23-33. <https://doi.org/10.2147/PLMI.S59826>
- Garcia-Garcia, A., Orts-Escolano, S., Oprea, S., Villena-Martinez, V., & Garcia-Rodriguez, J. (2017). A review on deep learning techniques applied to semantic segmentation. *Cornell University*. <https://doi.org/arXiv:1704.06857>
- Guo, Y., Liu, Y., Oerlemans, A., Lao, S., Wu, S., & Lew, M. S. (2016). Deep learning for visual understanding: A review. *Neurocomputing*, 187, 27-48. <https://doi.org/10.1016/j.neucom.2015.09.116>
- Hannig, J., Schäfer, H., Ackermann, J., Hebel, M., Schäfer, T., Döring, C., Hartmann, S., Hansmann, M.-L., & Koch, I. (2020). Bioinformatics analysis of whole slide images reveals significant neighborhood preferences of tumor cells in Hodgkin lymphoma. *PLOS Computational Biology*, 16(1), e1007516. <https://doi.org/10.1371/journal.pcbi.1007516>
- Hou, L., Samaras, D., Kurc, T. M., Gao, Y., Davis, J. E., & Saltz, J. H. (2016). *Patch-Based Convolutional Neural Network for Whole Slide Tissue Image Classification*. Proceedings of the IEEE conference on computer vision and pattern recognition.
- Howard, A. G. (2013). Some improvements on deep convolutional neural network based image classification. *Cornell University*. <https://doi.org/arXiv:1312.5402>
- Joseph, J., Roudier, M. P., Narayanan, P. L., Augulis, R., Ros, V. R., Pritchard, A., Gerrard, J., Laurinavicius, A., Harrington, E. A., & Barrett, J. C. (2019). Proliferation tumour marker

- network (PTM-NET) for the identification of tumour region in Ki67 stained breast cancer whole slide images. *Scientific Reports*, 9(1), 1-12. <https://doi.org/10.1038/s41598-019-49139-4>
- Kallenberg, M., Petersen, K., Nielsen, M., Ng, A. Y., Diao, P., Igel, C., Vachon, C. M., Holland, K., Winkel, R. R., & Karssemeijer, N. (2016). Unsupervised deep learning applied to breast density segmentation and mammographic risk scoring. *IEEE Transactions on Medical Imaging*, 35(5), 1322-1331. <https://doi.org/10.1109/TMI.2016.2532122>
- Karpathy, A., Johnson, J., & Fei-Fei, L. (2015). Visualizing and understanding recurrent networks. *Cornell University*. <https://doi.org/arXiv:1506.02078>
- Khan, R. N., Parvaiz, M. A., Khan, A. I., & Loya, A. (2019). Invasive carcinoma in accessory axillary breast tissue: A case report. *International Journal of Surgery Case Reports*, 59, 152-155. <https://doi.org/10.1016/j.ijscr.2019.05.037>
- Kumar, N., Gupta, R., & Gupta, S. (2020). Whole slide imaging (WSI) in pathology: Current perspectives and future directions. *Journal of Digital Imaging*, 33, 1034-1040. <https://doi.org/10.1007/s10278-020-00351-z>
- LeCun, Y., Huang, F. J., & Bottou, L. (2004). *Learning Methods for Generic Object Recognition with Invariance to Pose and Lighting*. Proceedings of the 2004 IEEE Computer Society Conference on Computer Vision and Pattern Recognition.
- Lee, S., Amgad, M., Masoud, M., Subramanian, R., Gutman, D., & Cooper, L. (2019). *An Ensemble-Based Active Learning for Breast Cancer Classification*. 2019 IEEE International Conference on Bioinformatics and Biomedicine (BIBM),
- Lee, S., Amgad, M., Mobadersany, P., McCormick, M., Pollack, B. P., Elfandy, H., Hussein, H., Gutman, D. A., & Cooper, L. A. (2021). Interactive classification of whole-slide imaging

- data for cancer researchers. *Cancer Research*, 81(4), 1171-1177.
<https://doi.org/10.1158/0008-5472.CAN-20-0668>
- Lee, S., Farley, C., Shim, S., Yoo, W.-S., Zhao, Y., & Choi, W. (2020). *Unsupervised Learning of Deep-Learned Features from Breast Cancer Images*. 2020 IEEE 20th International Conference on Bioinformatics and Bioengineering (BIBE),
- Liu, X., Deng, Z., & Yang, Y. (2019). Recent progress in semantic image segmentation. *Artificial Intelligence Review*, 52(2), 1089-1106. <https://doi.org/10.1007/s10462-018-9641-3>
- Long, J., Shelhamer, E., & Darrell, T. (2015). *Fully Convolutional Networks for Semantic Segmentation*. Proceedings of the IEEE Conference on Computer Vision and Pattern Recognition,
- Luveta, J., Parks, R. M., Heery, D. M., Cheung, K.-L., & Johnston, S. J. (2020). Invasive lobular breast cancer as a distinct disease: Implications for therapeutic strategy. *Oncology and Therapy*, 8(1), 1-11. <https://doi.org/10.1007/s40487-019-00105-0>
- Marée, R., Rollus, L., Stévens, B., Hoyoux, R., Louppe, G., Vandaele, R., Begon, J.-M., Kainz, P., Geurts, P., & Wehenkel, L. (2016). Collaborative analysis of multi-gigapixel imaging data using cytomine. *Bioinformatics*, 32(9), 1395-1401.
<https://doi.org/10.1093/bioinformatics/btw013>
- Murthy, V., Hou, L., Samaras, D., Kurc, T. M., & Saltz, J. H. (2017). *Center-Focusing Multi-Task CNN with Injected Features for Classification of Glioma Nuclear Images*. 2017 IEEE Winter Conference on Applications of Computer Vision (WACV).

- Nalisnik, M., Amgad, M., Lee, S., Halani, S. H., Vega, J. E. V., Brat, D. J., Gutman, D. A., & Cooper, L. A. (2017). Interactive phenotyping of large-scale histology imaging data with HistomicsML. *Scientific Reports*, 7(1), 1-12. <https://doi.org/10.1038/s41598-017-15092-3>
- Ordóñez, F. J., & Roggen, D. (2016). Deep convolutional and LSTM recurrent neural networks for multimodal wearable activity recognition. *Sensors*, 16(1), 115. <https://doi.org/10.3390/s16010115>
- Ronao, C. A., & Cho, S.-B. (2016). Human activity recognition with smartphone sensors using deep learning neural networks. *Expert Systems with Applications*, 59, 235-244. <https://doi.org/10.1016/j.eswa.2016.04.032>
- Ronneberger, O., Fischer, P., & Brox, T. (2015). *U-net: Convolutional Networks for Biomedical Image Segmentation*. International Conference on Medical Image Computing and Computer-Assisted Intervention,
- Senaras, C., Niazi, M. K. K., Lozanski, G., & Gurcan, M. N. (2018). DeepFocus: Detection of out-of-focus regions in whole slide digital images using deep learning. *PLOS ONE*, 13(10), e0205387. <https://doi.org/10.1371/journal.pone.0205387>
- Serag, A., Ion-Margineanu, A., Qureshi, H., McMillan, R., Saint Martin, M.-J., Diamond, J., O'Reilly, P., & Hamilton, P. (2019). Translational AI and deep learning in diagnostic pathology. *Frontiers in Medicine*, 6(185). <https://doi.org/10.3389/fmed.2019.00185>
- Settles, B. (2009). Active Learning literature survey. *University of Wisconsin–Madison*. <http://digital.library.wisc.edu/1793/60660>
- Settles, B. (2011). *From Theories to Queries: Active Learning in Practice*. Active Learning and Experimental Design workshop In conjunction with AISTATS 2010,

- Sharma, N., Jain, V., & Mishra, A. (2018). An analysis of convolutional neural networks for image classification. *Procedia Computer Science*, 132, 377-384.
<https://doi.org/10.1016/j.procs.2018.05.198>
- Siegel, R. L., Miller, K. D., & Jemal, A. (2020). Cancer statistics, 2020. *CA: A Cancer Journal for Clinicians*, 70(1), 7-30. <https://doi.org/10.3322/caac.21590>
- Smith, R. A., Andrews, K. S., Brooks, D., Fedewa, S. A., Manassaram-Baptiste, D., Saslow, D., & Wender, R. C. (2019). Cancer screening in the United States, 2019: A review of current American Cancer Society guidelines and current issues in cancer screening. *CA: A Cancer Journal for Clinicians*, 69(3), 184-210. <https://doi.org/10.3322/caac.21557>
- Sullivan, L. (2016). Survival analysis. *Boston University, School of Public Health*.
- Sun, W., Zheng, B., & Qian, W. (2017). Automatic feature learning using multichannel ROI based on deep structured algorithms for computerized lung cancer diagnosis. *Computers in Biology and Medicine*, 89, 530-539.
- Tai, S., & Lo, Y. (2018, 19-21 Sept. 2018). *Using Deep Learning to Evaluate the Segmentation of Liver Cell from Biopsy Image*. 2018 9th International Conference on Awareness Science and Technology (iCAST),
- Wang, L., Qiao, Y., & Tang, X. (2015). *Action Recognition with Trajectory-Pooled Deep-Convolutional Descriptors*. Proceedings of the IEEE Conference on Computer Vision and Pattern Recognition.
- Wang, S., Yang, D. M., Rong, R., Zhan, X., & Xiao, G. (2019). Pathology image analysis using segmentation deep learning algorithms. *The American Journal of Pathology*, 189(9), 1686-1698. <https://doi.org/10.1016/j.ajpath.2019.05.007>

- Wen, S., Kurc, T. M., Hou, L., Saltz, J. H., Gupta, R. R., Batiste, R., Zhao, T., Nguyen, V., Samaras, D., & Zhu, W. (2018). Comparison of different classifiers with Active Learning to support quality control in nucleus segmentation in pathology images. *AMIA Joint Summits on Translational Science, 2017*, 227-236.
<https://pubmed.ncbi.nlm.nih.gov/29888078>
- Xu, L., Ren, J. S., Liu, C., & Jia, J. (2014). Deep convolutional neural network for image deconvolution. *Advances in Neural Information Processing Systems, 27*, 1790-1798.
http://www.cse.cuhk.edu.hk/leojia/papers/deconv_nips14.pdf
- Xu, Y., Jia, Z., Wang, L.-B., Ai, Y., Zhang, F., Lai, M., Eric, I., & Chang, C. (2017). Large scale tissue histopathology image classification, segmentation, and visualization via deep convolutional activation features. *BMC Bioinformatics, 18*(1), 1-17.
<https://doi.org/10.1186/s12859-017-1685-x>
- Yao, J., Zhu, X., Jonnagaddala, J., Hawkins, N., & Huang, J. (2020). Whole slide images based cancer survival prediction using attention guided deep multiple instance learning networks. *Medical Image Analysis, 65*, 101789.
<https://doi.org/10.1016/j.media.2020.101789>
- Yu, K., Zhang, C., Berry, G., Altman, R., Ré, C., Rubin, D., & Snyder, M. (2016). Predicting non-small cell lung cancer prognosis by fully automated microscopic pathology image features. *Nature Communications 7*: 12474. <https://doi.org/10.1038/ncomms12474>
- Zhang, H., Dana, K., Shi, J., Zhang, Z., Wang, X., Tyagi, A., & Agrawal, A. (2018). *Context Encoding for Semantic Segmentation*. Proceedings of the IEEE Conference on Computer Vision and Pattern Recognition,

Zhu, X., Yao, J., Zhu, F., & Huang, J. (2017). *Wsisia: Making Survival Prediction from Whole Slide Histopathological Images*. Proceedings of the IEEE Conference on Computer Vision and Pattern Recognition,

APPENDIX A: APPROVAL LETTER



Office of Research Integrity

March 11, 2021

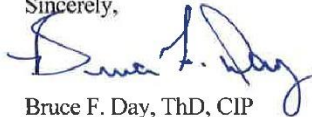
Vishwanshi Nilkamal Joshi
2615 3rd Ave.
Huntington, WV 25702

Dear Ms. Joshi:

This letter is in response to the submitted thesis abstract entitled "*The U-Net Based Active Learning Framework for Enhancing Cancer Immunotherapy.*" After assessing the abstract, it has been deemed not to be human subject research and therefore exempt from oversight of the Marshall University Institutional Review Board (IRB). The Code of Federal Regulations (45CFR46) has set forth the criteria utilized in making this determination. Since the information in this study does not involve human subjects as defined in the above referenced instruction, it is not considered human subject research. If there are any changes to the abstract you provided then you would need to resubmit that information to the Office of Research Integrity for review and a determination.

I appreciate your willingness to submit the abstract for determination. Please feel free to contact the Office of Research Integrity if you have any questions regarding future protocols that may require IRB review.

Sincerely,



Bruce F. Day, ThD, CIP
Director

WE ARE... MARSHALL.

One John Marshall Drive • Huntington, West Virginia 25755 • Tel 304/696-4303
A State University of West Virginia • An Affirmative Action/Equal Opportunity Employer

APPENDIX B: ACRONYMS

AUC	Area Under the Curve
CNN	Convolutional Neural Network
DCNN	Deep Convolutional Neural Network
FPR	False Positive Rate
ROC	Receiver Operator Characteristic
TCGA-BRCA	Cancer Genome Atlas Breast Invasive Carcinoma
TIL	Tumor-Infiltrating Lymphocytes
TPR	True Positive Rate
WSI	Whole Slide Image